

Proceeding Paper

# Chemical Transformation of Typical Biological Recognition Elements in Reactions with Nanosized Targets: A Study of Glutathione Coated Silver Nanoparticles <sup>†</sup>

Sergii Kravchenko \*, Praskoviya Boltovets and Boris Snopok 

V.E. Lashkaryov Institute of Semiconductor Physics, National Academy of Sciences of Ukraine, 03028 Kyiv, Ukraine; boltovets@isp.kiev.ua (P.B.); snopok@isp.kiev.ua (B.S.)

\* Correspondence: kravchenko@isp.kiev.ua

<sup>†</sup> Presented at the 3rd International Electronic Conference on Biosensors, 8–21 May 2023;

Available online: <https://iecb2023.sciforum.net>.

**Abstract:** Glutathione (GT) is a complexing agent that plays a key role in the functioning of a living cell. Gold nanoparticles are often used as transducers of nanosized biosensors, since they have the optical and chemical properties necessary for sensory applications, and make it possible to form a sensitive layer with the desired recognition element. Silver nanoparticles (AgNPs) also have attracted increasing interest to sensor applications due to the narrower plasmon resonance band compared to gold nanoparticles, but different surface chemistry. The purpose of this study is to provide an information about GT-coated AgNPs evolution as a system consisting of AgNPs transducer and GT recognition element. AgNPs are transformed through Ag<sup>+</sup> to amorphous Ag, while GT promotes AgNPs to be dissolved, and gets decomposed by reactive oxygen species (ROS) during the transformation.

**Keywords:** silver nanoparticles; nanostructured carbon; glutathione; local plasmon; ROS



**Citation:** Kravchenko, S.; Boltovets, P.; Snopok, B. Chemical Transformation of Typical Biological Recognition Elements in Reactions with Nanosized Targets: A Study of Glutathione Coated Silver Nanoparticles. *Eng. Proc.* **2023**, *35*, 31. <https://doi.org/10.3390/IECB2023-14571>

Academic Editor: Sara Tombelli

Published: 8 May 2023



**Copyright:** © 2023 by the authors. Licensee MDPI, Basel, Switzerland. This article is an open access article distributed under the terms and conditions of the Creative Commons Attribution (CC BY) license (<https://creativecommons.org/licenses/by/4.0/>).

## 1. Introduction

The study of the interaction between biologically significant molecules and nanoparticles attracts interest in connection with their application in sensors, biosensors, and biomedical diagnostics. In addition to their practical applications in medicine and pharmacology, they are used in fundamental research carried out in studying processes that occur in biological systems [1]. One of the biological molecules that play a key role in biological processes is glutathione (GT). This molecule is a tripeptide one, having the structure as L-glutamine-L-cysteine-glycine ( $\gamma$ -Glu-Cys-Gly), and performs intra- and intercellular transport of metal ions and cellular protection in biological systems. Due to its unique properties, GT is used as an important defensive mean against ROS, xenobiotic metabolites, and heavy metals to protect living cells from the destructive factors [2]. The realization of this function is possible due to the presence of active functional groups, such as COOH, SH, NH<sub>2</sub>, in the GT molecule and its conformational flexibility.

Gold nanoparticles (AuNPs) are often used as transducers of nanosized biosensors, since they have the optical and chemical properties necessary for sensory applications and make it possible to form a sensitive layer with the desired functionality on its surface using various molecular recognition species, in particular GT molecule [3]. Due to the presence of SH group in the molecule, direct irreversible GT immobilization on the gold surface occurs at room temperature without any additional activation procedures. Thus, GT-stabilized AuNPs showed extremely high renal clearance while at the same time exhibiting good stability in the blood stream. Moreover, GT-coated AuNPs led to a new class of inorganic nanoscale carriers which can deliver drugs to or directly affect the tumor under the influence of external factors (i.e., electromagnetic field) [4].

Silver nanoparticles (AgNPs) also have attracted increasing interest to sensor applications due to different spectral range, typically the narrower plasmon resonance band compared to AuNPs, agglomeration behavior, but different surface chemistry. Thus, GT-conjugated AgNPs are characterized by the presence of circular dichroism, which indicates the instability of the GT attachment to the silver surface [5,6]. The purpose of this study is to provide an information of GT-coated AgNPs evolution as a system consisting of AgNPs transducer and GT recognition element.

## 2. Materials and Methods

AgNPs (<100 nm, 10% wt) in ethylene glycol, Glutathione (99%), Sodium carbonate (>99, 5%), and Sodium bicarbonate (>99, 7%) were received from Sigma-Aldrich. The optical absorbance was studied by UV-Vis spectroscopy on Umico SQ2800 (UNICO, Dayton, NJ, USA). The nanoparticle morphology was studied using JEM 1011 TEM (JEOL, Tokyo, Japan) at an accelerating voltage of 100 kV. Raman spectra were measured using a confocal system (NTEGRA Spectra, NT-MDT, Apeldoorn, Netherlands) and a laser source (GL, 532 nm, model LCM-S-111). A partially focused laser beam with a diameter of ~5  $\mu\text{m}$  was used, the laser radiation intensity was ~50  $\mu\text{W}/\mu\text{m}^2$  in the sample plane, and the integration time was 10 s.

## 3. Results

### 3.1. Transformation in 3 Days

A 0.01 M carbonate buffer solution (pH~10) was used to prepare the AgNPs buffer solution and the GT one. First, a 5 mM AgNPs buffer solution was prepared by mixing the initial AgNPs (10% wt) in ethylene glycol with carbonate buffer solution in terms of the silver amount. Then, GT solutions were prepared in carbonate buffer at concentrations of 20, 2, 0.2, and 0.02 mM. The AgNPs buffer solution and the GT one (with a certain GT concentration) were mixed in equal volumes. The optical absorbance of the obtained solutions was measured in 10 min, 1 h, and 3 days after mixing, the resulting solutions being stored at room temperature under daylight exposition.

Uv-Vis spectroscopy study showed the presence of a definite peak at ~408 nm, corresponding to Ag plasmon band, is characteristic for all mixtures in ten minutes after the experiment beginning (Figure 1a). Interestingly, the new peak appeared at 550–600 nm immediately in 10 min after mixing 20 mM GT solution (maximum concentration), which indicated the AgNPs cluster formation in the solution.

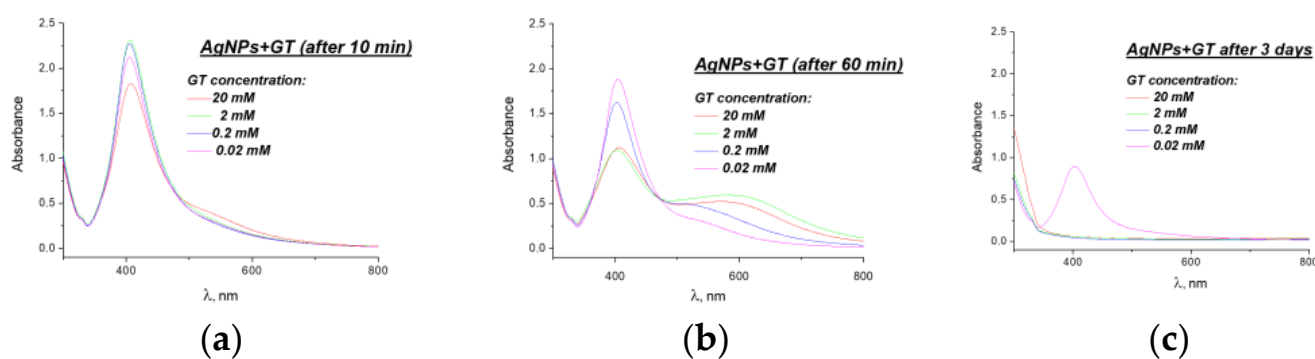
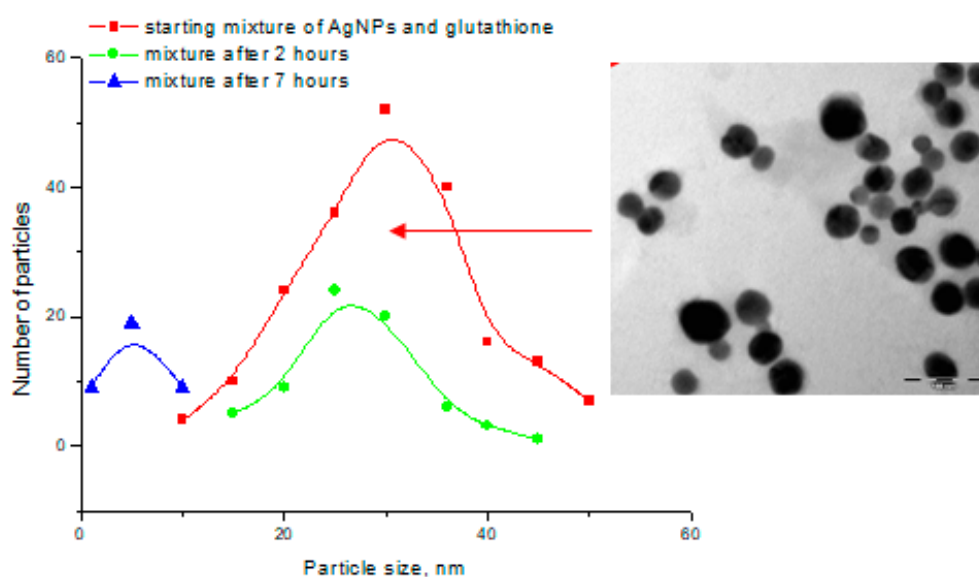


Figure 1. UV-Vis spectra of [AgNPs]GT: (a) after 60 min; (b) after 10 min; (c) after 3 days.

One hour after mixing the characteristic absorbance, changes in the long-wavelength band were observed for all the mixtures under study, and the expression degree of such an absorbance change (according to the spectra) clearly depended on the GT concentration in the solution. The intensity of the local plasmon peak naturally was decreasing with the increase in the number of clusters (Figure 1b). The disappearance of the band at 408 nm

and in the long-wavelength region was observed in 3 days after mixture preparation, which indicated the absence of AgNPs with the size of more than 10 nm in solution (Figure 1c).

The observed changes are also confirmed by the results obtained from the study of the [AgNPs]GT mixture by TEM (Figure 2). The [AgNPs]GT was prepared by mixing equal volumes of 5 mM AgNPs and 20 mM GT buffer solutions. TEM images were obtained: (1) immediately after mixture preparation, (2) after 2 h, and (3) after 7 h. On the base of the obtained images, AgNPs appear to form nanoparticle clusters due to the GT molecules. The nanoparticles size in clusters was found to decrease with time, i.e., the maximum mean size of AgNPs in the solution at the beginning was ~36 nm, then, it changed to ~27 nm in 2 h, and finally, it reached ~7 nm in 7 h.



**Figure 2.** Size distribution of AgNPs during the time.

The solution under investigation has been kept for a while in refrigerator at +8 °C.

### 3.2. Transformation in Six Months

An insoluble black precipitate was found after six months of keeping. The Raman spectra of the precipitate had two intense vibrational modes in the range from ~800 to ~2100  $\text{cm}^{-1}$  (Figure A1a), and several low-intensive ones in the range from ~2100 to ~3600  $\text{cm}^{-1}$  (Figure A1b).

It is known that the Raman spectra of crystalline graphite contain a single intense one-phonon band G (*graphite*) with a center of ~1580  $\text{cm}^{-1}$  and a full width at half maximum (FWHM) of ~13  $\text{cm}^{-1}$  [7]. At the same time, there are D (*disorder*) bands along with the G band in the spectra of defective and polycrystalline graphite, as well as various activated carbon materials [8]. Further, in the Raman spectra of crystalline graphite there is a two-phonon 2D band with a maximum at ~2700  $\text{cm}^{-1}$  along with the one-phonon G band. It should be noted that the Raman spectra of ideal graphene contain the vibrational mode of the one-phonon G band, which is about four times more intense than the two-phonon 2D band [9].

In the Raman spectra of the sample under investigation, the presence of the G band at 1585  $\text{cm}^{-1}$  indicates the presence of unoxidized  $\text{sp}^2$ -hybridized carbon atoms. A noticeable difference in the width and Raman shift of the G band in the spectra of the sample compared to crystalline graphite indicates a short length of the layered coherence of the carbon structure and small sizes of the  $\text{sp}^2$  "islands" [10]. On the other hand, the presence of an intense D band in the spectra indicates a high content of defects in the sample, in particular, oxidized regions in the carbon matrix. It should also be noted that the intensity of the

one-phonon G band is only twice as high as the intensity of the two-phonon 2D band (i.e., graphene structure in the sample is absent). The results obtained indicate that the insoluble solid that precipitated from the solution is nanostructured oxidized graphite.

The study of the mother solution obtained after precipitate separation by Raman spectroscopy exhibited the presence of silver compounds along with the presence of certain organic fragments, some of which belong to the GT molecule (Figure A2). Thus, the Raman spectra contain vibrational modes  $\nu(\text{Ag-N})$  at  $346\text{ cm}^{-1}$  (symm. stretching),  $\nu(\text{Ag-S})$  at  $188\text{ cm}^{-1}$ ,  $243\text{ cm}^{-1}$  and  $273\text{ cm}^{-1}$  (stretching mode),  $\nu(\text{C-O-Ag})$  at  $258\text{ cm}^{-1}$ ,  $341\text{ cm}^{-1}$  and  $490\text{ cm}^{-1}$  (bending mode),  $\nu(\text{C=O})$  at  $614\text{ cm}^{-1}$  and  $664\text{ cm}^{-1}$  (bending mode),  $\nu(\text{CO-O})$  at  $1230\text{ cm}^{-1}$  (stretching mode),  $\nu(\text{O-C-O})$  at  $1346\text{ cm}^{-1}$  (symm. stretching), and  $1536\text{ cm}^{-1}$  (asymm. stretching) [11,12]. It can be assumed that the solution contains  $\text{Ag}_2\text{S}$ , carboxyl silver salts  $\text{RCOOAg}$ , and complex compounds of silver ions with amino acid residues  $-\text{OOC}(\text{R})\text{C}(\text{NH}_2)\text{Ag}^+$ , along with GT molecules. It should be noted that a long exposure of the sample under the laser beam leads to the appearance of new vibrational modes  $\nu(\text{N-O})$  at  $1030\text{ cm}^{-1}$  (symm. stretching),  $1330\text{ cm}^{-1}$  (asymm. stretching) and  $\nu(\text{S-O})$  at  $970\text{ cm}^{-1}$  (symm. stretching), and  $1080\text{ cm}^{-1}$  (asymm. stretching) (Figure A3). In addition, photodecomposition of light-sensitive  $\text{Ag}_2\text{S}$  occurs as a result of exposure under light, as evidenced by the appearance of vibrational modes at  $490$ ,  $1250$ , and  $1435\text{ cm}^{-1}$ .

### 3.3. Transformation in a Year

After the next 6 months, the precipitation of an insoluble black precipitate from the solution was again found. Raman studies have not made it possible to determine its composition. When mixed with dilute nitric acid, insoluble precipitate dissolved. Therefore, presumably, this precipitate can be amorphous silver. Unfortunately, there is no possibility to perform an  $\text{Ag}^+$  test evaluation by means of chloride anions due to the low concentration of  $\text{Ag}^+$  ions in the solution.

## 4. Discussion

### 4.1. Evolution of $[\text{AgNPs}]\text{GT}$ Mixture

$\text{AgNPs}$  in  $[\text{AgNPs}]\text{GT}$  mixture decreases in size over time due to the diffusion of silver ions in solution (Figure A4). Then, an insoluble precipitate is formed in the solution, which is found to be a nanostructured carbon compound-oxidized nanostructured graphite. This indicates that regions with extremely high reactivity appear in the solution, in which the oxidation and decomposition of organic molecules occur. In addition, oxidation of GT functional groups is observed when the sample is exposed to light (in the Raman study), which also indicates the presence of regions with extremely high reactivity.

Such an effect occurs only when two plasmonic particles approach each other at a distance of  $< 5\text{ nm}$ , which leads to an increase in the electromagnetic field in the region between them due to the local plasmon resonance of the nanoparticle and the incident light radiation [13]. In our case, the approximation of  $\text{AgNPs}$  is due to the nanoparticles clustering by reason of GT grafting to the  $\text{AgNPs}$  surface.

### 4.2. Chemical Transformation in $[\text{AgNPs}]\text{GT}$ Mixture (Figure A5)

The choice of carbonate buffer (pH~10) for the preparation of buffer solutions of  $\text{AgNPs}$  and GT was due to two factors. On the one hand, the dispersed phase is characterized by having a significant specific surface area, and hence it has an excess of surface energy. The tendency of the thermodynamic system to a minimum of energy causes a certain orientation of molecules, ions, and electrons in the surface layer, which leads to the appearance of an electric charge on the surface of nanoparticles and the formation of an electrical double layer (EDL) on it. In the case of  $\text{AgNPs}$ ,  $\text{Ag}^+$  is transferred to the solution, the solid surface of the nanoparticle is charged negatively, and the dispersed medium is charged positively, with the fixation of a certain zeta-potential. The presence of  $\text{OH}^-$  anions in a colloidal solution, due to their high polarizability, leads to increasing in the thickness of the diffusion layer where  $\text{Ag}^+$  is diffused. On the other hand, GT is

characterized by the presence of functional groups that have an affinity for  $\text{Ag}^+$  (COOH, SH and  $\text{NH}_2$ ).  $\text{pK}_a$  values for GT are as follow:  $\text{pK}_a$  (COOHGlu) = 2.3,  $\text{pK}_a$  ( $\text{NH}_2$ Glu) = 9.65,  $\text{pK}_a$  (SHCys) = 2.3, and  $\text{pK}_a$  (COOHGly) = 3.7 [14]. Thus, thanks to the carbonate buffer, the necessary parameters of EDL, ionization of COOH and SH and deprotonation of  $\text{NH}_2$  groups, are provided.

The  $\text{Ag}^+$  is characterized by a high binding affinity to the sulfur atom in the GT molecule (binding constant  $K_b = 12.3$ ) and their interaction leads to the formation of  $\text{Ag}^+\text{GTS}^-$  in the form of a polymer compound with a layered structure, in which the hydrophilic fragments of GT lie perpendicularly on both sides of the plane of the formed framework [15]. During the subsequent oxidative degradation, this polymer layer is converted into a  $\text{Ag}_2\text{S}$  passivation layer. It should be noted that if aqueous solutions of silver nanoparticles are mixed with aqueous solutions of  $\text{Na}_2\text{S}$ , a  $\text{Ag}_2\text{S}$  passivation layer is also formed, but the nanoparticles do not decrease in size when associating with each other [16].

In our case, the amino acids that make up glutathione (Glu and Gly) bind to  $\text{Ag}^+$  (complex formation) and remove ions from the equilibrium medium, which provides to further ionization of the nanoparticle surface [17]. The nanoparticle size decreases, with a corresponded increasing in dispersion and specific surface area, which, in turn, leads to the intensification of  $\text{Ag}^+$  release from the nanoparticle surface. However, this process proceeds to a certain limit, until the formation of stable, so-called, “magic clusters” of silver [18].

Nanocomposite carbon is formed due to the decomposition of organic molecules in the region of so-called “hot spots”, in which the electric field of incident light radiation is significantly enhanced due to resonance with oscillations of local plasmon in nanoparticles [13]. Further, regions with increased electric field cause the oxidation of SH and  $\text{NH}_2$ -groups into  $\text{SO}_4^{2-}$  and  $\text{NO}_3^-$  anions, respectively.

Therefore, the effect of light on the composition has a twofold effect: it promotes the oxidative ionization of silver (dissolution of nanoparticles) and its photoreduction (formation of nanoparticles).

## 5. Conclusions

- Chemical transformation of glutathione coated silver nanoparticles undergoes complex changes in time.
- AgNPs are transformed through  $\text{Ag}^+$  to amorphous Ag (*reductio argenti artificis ad argentum primordiale*).
- GT provides the approximation of AgNPs with the formation of high intensive electrical field regions between them due to vibration resonance of incident light and local plasmon in nanoparticles. Reactive oxygen species (ROS) formation occurs in these regions as observed in living systems. GT promotes AgNPs to be dissolved and gets decomposed by ROS during the transformation.
- Light irradiation plays the key role in this kind of transformation. As it has been absent the transformation of [AgNPs]GT results in “majority of Ag remains in the form of AgNPs and that 23% is present as  $\text{Ag}_2\text{S}$  in soil; in both root and nodule tissues,  $\text{Ag-GSH}$  is the main component (40.6–88%) other than AgNPs (12–59.4%) [19].
- The transformation mechanism presents the possibility in prognosis of processes occurred in different media when using AgNPs for sensors, pharmaceutical, medical, and agricultural applications.

**Author Contributions:** Conceptualization, S.K. and B.S.; methodology, B.S.; validation, S.K. and B.S.; investigation, P.B. and S.K.; resources, P.B.; data curation, P.B.; writing—original draft preparation, S.K.; writing—review and editing, S.K.; visualization, P.B.; supervision, B.S.; project administration, B.S.; funding acquisition, B.S. All authors have read and agreed to the published version of the manuscript.

**Funding:** This research received no external funding.

**Institutional Review Board Statement:** Not applicable.

**Informed Consent Statement:** Not applicable.

**Data Availability Statement:** Data are available on request.

**Conflicts of Interest:** The authors declare no conflict of interest.

**Appendix A**

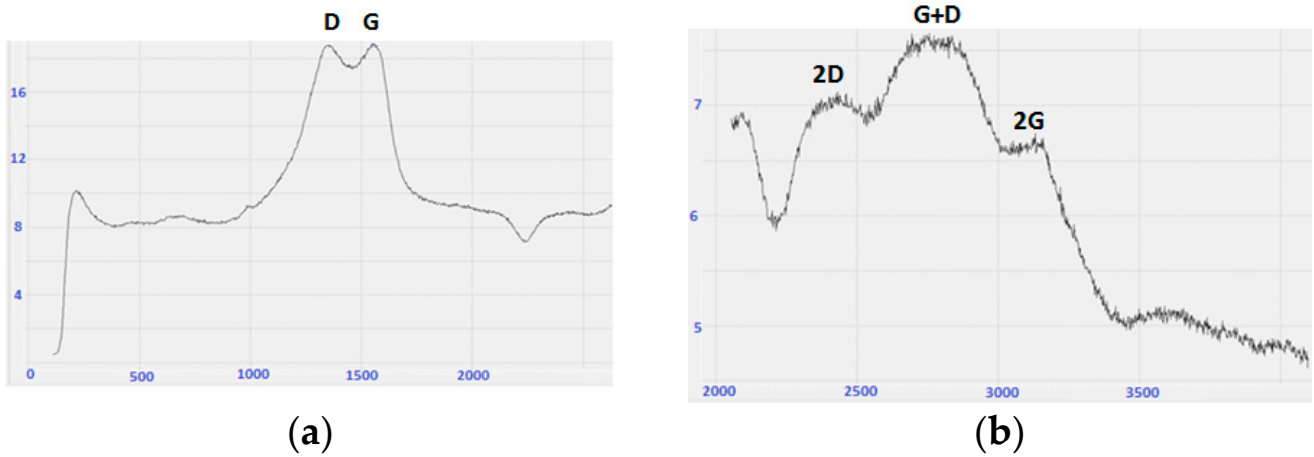


**Figure A1.** Raman spectra of solid precipitated from [AgNPs]GT mixture: (a) phonon G band; (b) phonon 2D band.

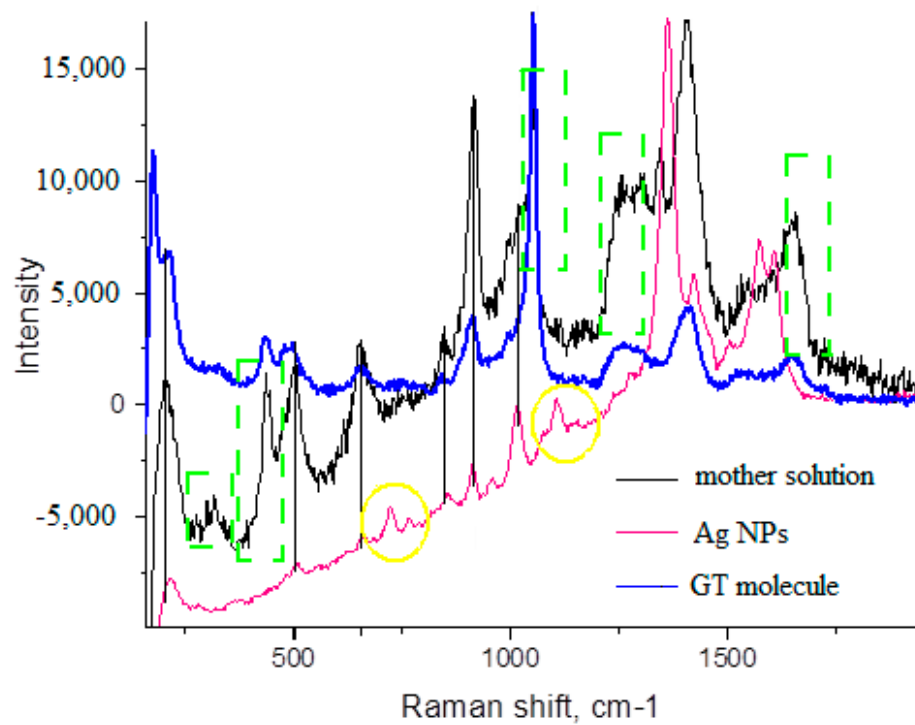


**Figure A2.** Raman spectra of mother solution (yellow circles—bands absent in the mother solution; green dotted squares—GT molecule bands).

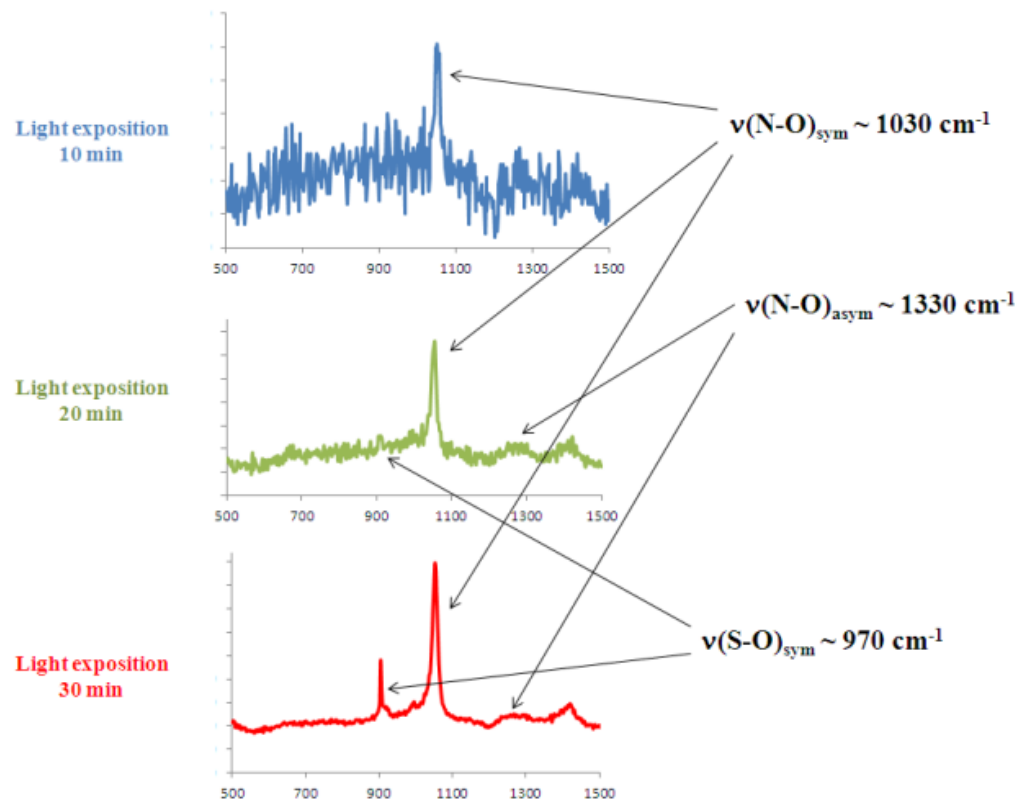


Figure A3. Raman spectra of mother solution after light exposition during the definite time.

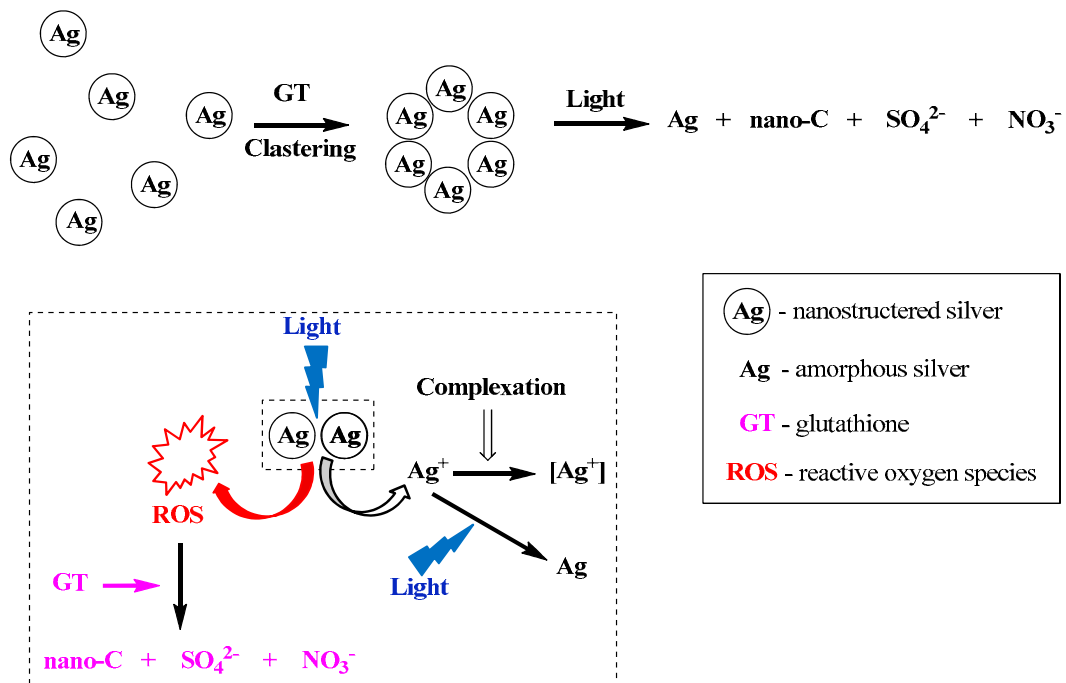


Figure A4. Evolution of [AgNPs]GT mixture.

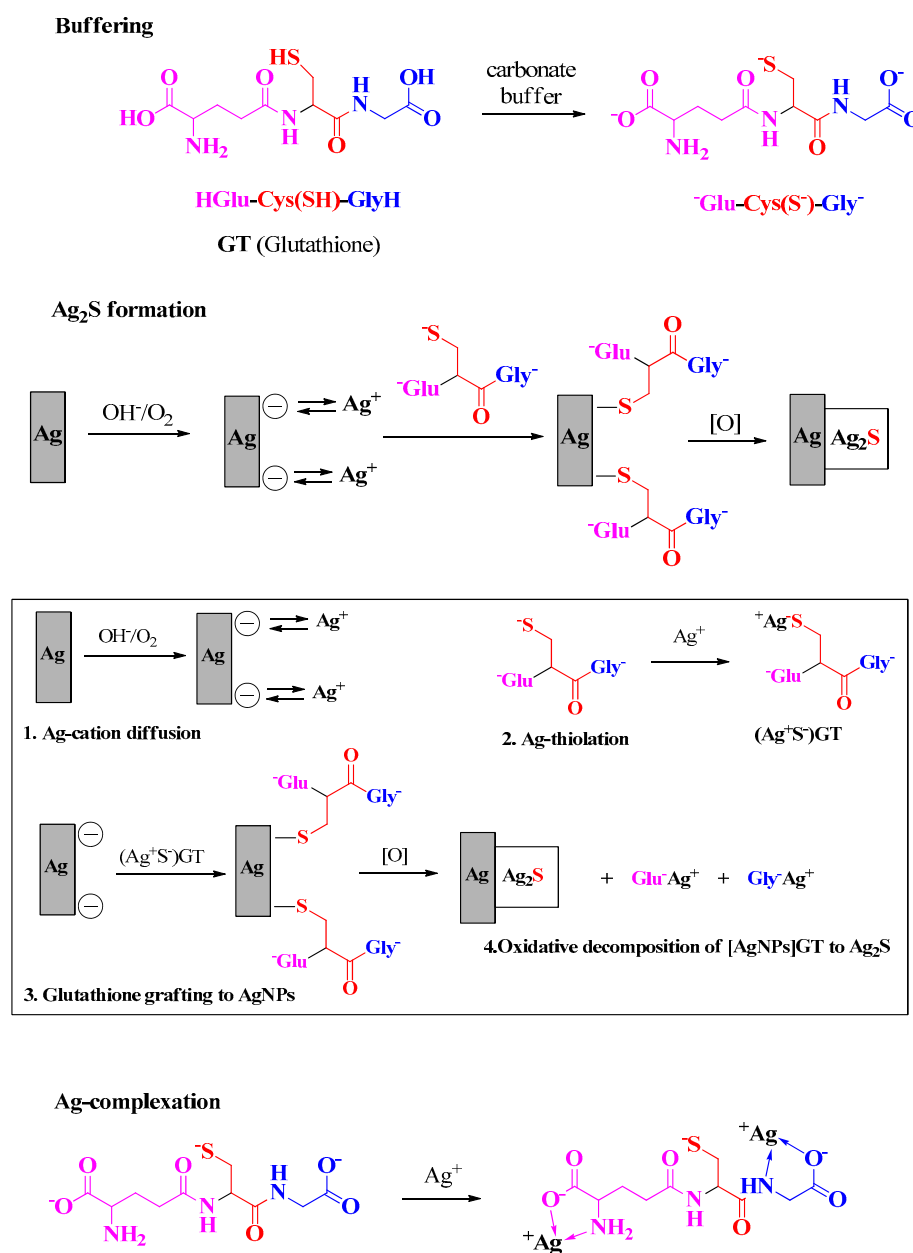


Figure A5. Chemical transformation in [AgNPs]GT mixture.

## References

- Ramesh, M.; Janani, R.; Deepa, C.; Rajeshkumar, L. Nanotechnology-Enabled Biosensors: A Review of Fundamentals, Design Principles, Materials, and Applications. *Biosensors* **2023**, *13*, 40. [[CrossRef](#)] [[PubMed](#)]
- Vašková, J.; Kočan, L.; Vaško, L.; Perjési, P. Glutathione-Related Enzymes and Proteins: A Review. *Molecules* **2023**, *28*, 1447. [[CrossRef](#)] [[PubMed](#)]
- Ferrari, E. Gold Nanoparticle-Based Plasmonic Biosensors. *Biosensors* **2023**, *13*, 411. [[CrossRef](#)] [[PubMed](#)]
- Yu, M.; Xu, J.; Zheng, J. Renal Clearable Luminescent Gold Nanoparticles: From the Bench to the Clinic. *Angew. Chem. Int. Ed. Engl.* **2019**, *58*, 4112. [[CrossRef](#)] [[PubMed](#)]
- Taihua, L.; Hyun, G.; Hee-Seung, L.; Seong-Ho, C. Circular dichroism study of chiral biomolecules conjugated with silver nanoparticles. *Nanotechnology* **2004**, *15*, S660.
- Digregorio, M.; Ben Moshe, A.; Tirosh, E.; Galantini, L.; Markovich, G. Chiroptical Study of Plasmon-Molecule Interaction: The Case of Interaction of Glutathione with Silver Nanocubes. *J. Phys. Chem. C* **2015**, *119*, 17111. [[CrossRef](#)]
- Tuinstra, F.; Koenig, J. Raman spectrum of graphite. *J. Chem. Phys.* **1970**, *53*, 1126. [[CrossRef](#)]
- Ferrari, A.; Robertson, J. Interpretation of Raman spectra of disordered and amorphous carbon. *Phys. Rev. B* **2000**, *61*, 14095. [[CrossRef](#)]

9. Cancado, L.; Reina, A.; Kong, J.; Dresselhaus, M. Geometrical approach for the study of G' band in the Raman spectrum of monolayer graphene, bilayer graphene, and bulk graphite. *Phys. Rev. B* **2008**, *77*, 245408. [[CrossRef](#)]
10. Jorio, A.; Souza Filho, A. Raman studies of carbon nanostructures. *Annu. Rev. Mater. Res.* **2016**, *46*, 357. [[CrossRef](#)]
11. Martina, I.; Wiesinger, R.; Jembrih-Simbürger, D.; Schreiner, M. Micro-Raman Spectroscopy of Silver Corrosion Products. *E-Preserv. Sci.* **2012**, *9*, 1.
12. Woidy, P.; Kraus, F. The Diammine Silver(I) Acetate [Ag(NH<sub>3</sub>)<sub>2</sub>]OAc. *Z. Anorg. Allg. Chem.* **2013**, *639*, 2643. [[CrossRef](#)]
13. Krishchenko, I.; Manoilov, E.; Kravchenko, S.; Snopok, B. Resonant Optical Phenomena in Heterogeneous Plasmon Nanostructures of Noble Metals: A Review. *Theor. Ex. Chem.* **2020**, *56*, 67. [[CrossRef](#)]
14. Matsui, R.; Ferran, B.; Oh, A.; Croteau, D.; Shao, D.; Han, J.; Pimentel, D.R.; Bachschmid, M. Redox Regulation via Glutaredoxin-1 and Protein S-Glutathionylation. *Antioxid. Redox Signal.* **2020**, *32*, 677. [[CrossRef](#)] [[PubMed](#)]
15. Odriozola, I.; Ormategui, N.; Loinaz, I.; Pomposo, J.A.; Grande, H.J. Coinage Metal–Glutathione Thiolates as a New Class of Supramolecular Hydrogelators. *Macromol. Symp.* **2008**, *266*, 96. [[CrossRef](#)]
16. Levard, C.; Reinsch, B.C.; Michel, F.M.; Oumahi, C.; Lowry, G.V.; Brown, G.E., Jr. Sulfidation Processes of PVP-Coated Silver Nanoparticles in Aqueous Solution: Impact on Dissolution Rate. *Environ. Sci. Technol.* **2011**, *45*, 5260. [[CrossRef](#)] [[PubMed](#)]
17. Démaret, A.; Abraham, F. Structure du L-[alpha]-alaninate d'argent. *Acta Cryst.* **1987**, *C43*, 1519. [[CrossRef](#)]
18. Kumar, S.; Michael, D.; Bolan, M.D.; Bigioni, T.P. Glutathione-Stabilized Magic-Number Silver Cluster Compounds. *J. Am. Chem. Soc.* **2010**, *132*, 13141. [[CrossRef](#)] [[PubMed](#)]
19. Ma, C.; Liu, H.; Chen, G.; Zhao, Q.; Guo, H.; Minocha, R.; Long, S.; Tang, Y.; Saad, E.; De La Torre, R.; et al. Dual roles of glutathione in silver nanoparticle detoxification and enhancement of nitrogen assimilation in soybean. *Environ. Sci. Nano* **2020**, *7*, 1954. [[CrossRef](#)]

**Disclaimer/Publisher's Note:** The statements, opinions and data contained in all publications are solely those of the individual author(s) and contributor(s) and not of MDPI and/or the editor(s). MDPI and/or the editor(s) disclaim responsibility for any injury to people or property resulting from any ideas, methods, instructions or products referred to in the content.